A Strategy to Prepare Wafer Scale Bismuth Compound Superstructures

*Chuan Fei Guo, Jianming Zhang, Meng Wang, Ye Tian, and Qian Liu**

The design and fabrication of well aligned nanostructures or super-nanostructures are of great interest in recent decades because such nanostructures are good units for electronic and photoelectric nanodevices including solar cells, nanogenerators, UV lasers, and field emission devices.[1–6] Directing the growth of nanostructures with a single crystalline (SC) epitaxial substrate has been a quite important strategy toward aligned, high-quality SC nanostructures.[3,7–11] Chemical vapor deposition (CVD) is a commonly used method for growing well aligned nanostructures on epitaxial substrates, for which a metallic thin film (typically gold) is often required, annealing at high temperatures to form metal nanoparticles as catalysts.[3,7–9,12] However, this method suffers from the fact that the metallic nanoparticles are not easy to remove after growth, as well as non-uniformity of products from zone to zone, and is therefore not suitable for large area nanodevices. An alternative method, solution growth directed by a seed layer on epitaxial substrate can grow well aligned 1D nanostructures without metal residues. For instance, Z. L. Wang et al. have successfully obtained vertically aligned ZnO nanorods from a ZnO seed layer on GaN substrate.[10] The success of fabricating arrays of 1D nanostructures has led to extensive investigation of their properties.

In the last decade, 2D nanostructures have attracted increasingly more attention. For example, 2D graphene has been one of the most attractive nanostructures for scientific research.[13,14] However, there are quite few works on the fabrication and properties of vertically aligned arrays of 2D nanostructures, many of which should be promising structures that may lead to practical applications.[11,15] We have previously reported that 2D orthogonal networks (2DONWs) of vertical BiOCl, $Bi_2O_2CO_3$, and β-Bi_2O_3 nanowalls, and nested 2DONWs (N2DONWs) of Bi_2S_3 nanowires are available via topotactic transformations with β-Bi_2O_3 thin films as the precursors.[16,17] The growth of such complex nanoarchitectures combines both bottom-up and top-down processes, and is directed by lattice match. This is a demonstration that nanostructures can be compatible with thin film technology and modern device fabrication processes. However, the scale of the vertical nanostructures is limited by the size of the precursors, the β-Bi_2O_3 domains, which are typically 20 μm in diameter. And there are only a small part of domains that can transform to vertical BiOCl networks. It is quite important to have the ability to grow well aligned 2D nanostructures on wafer scale, if we want to take full advantages of their properties and finally to apply them. The key to realize this purpose is to grow wafer scale SC β-Bi_2O_3 thin films. Herein, we show a route to SC β-Bi_2O_3 thin films, as well as the synthesis of wafer scale and well aligned BiOCl 2DONWs and Bi_2S_3 on $SrTiO_3$ (STO) substrate. The supernanostructures present anisotropic electrical property.

We have applied the crystallization of an amorphous BiO_x film on glass substrate to make the β-Bi_2O_3 thin film. BiO_x is a semiconductor with a bandgap of ~2 eV,[18] it often naturally forms on the surface of metallic bismuth nanostructures, with a thickness of several nanometers.[19] In this work, we use reactive sputtering to deposit flat BiO_x films, which could convert to β-Bi_2O_3 by thermal annealing at 300–600 °C for hours. Unfortunately, without lattice direction by SC substrate, the β-Bi_2O_3 thin film is always polycrystalline, with many SC domains in different crystallographic orientations. SC substrates have been proven to be effective for growing wafer scale and well aligned nanostructures owing to lattice direction. Thereupon we tried STO SC substrate, which has a cubic structure with lattice constant a = 3.905 Å, very close to the {200} interplanar spacing (3.871 Å) of β-Bi_2O_3. The lattice misfit between STO {100} and β-Bi_2O_3 {200} is

$$f = \frac{\left|d_{200|Bi_2O_3} - d_{100|STO}\right|}{d_{100|STO}} = 0.88\% \quad (1)$$

indicating that β-Bi_2O_3 could match well with STO. It is worth noting that we did the crystallization at 500 °C (actually crystallization begins at ~250 °C) rather than at room temperature, thus thermal expansion should be considered. X-ray diffraction (XRD) data show that from 25 to 500 °C, linear expansion of lattice parameter a for STO and β-Bi_2O_3 are 0.517% and 0.524% (supplementary information Figure S1), respectively. This tiny difference does not lead to significant change of lattice misfit at crystallization temperature, therefore it can be ignored.

We sputtered a 100–200 nm thick BiO_x thin film on (001)-oriented $SrTiO_3$ (STO) substrate, and then annealed

Dr. C. F. Guo, J. Zhang, M. Wang, Y. Tian, Prof. Q. Liu
National Center for Nanoscience and Technology,
China, No. 11 Beiyitiao Zhongguancun,
Beijing 100190, China
E-mail: liuq@nanoctr.cn
M. Wang, Prof. Q. Liu
TEDA Applied Physics School
Nankai University
Tianjin 300457, China

DOI: 10.1002/smll.201300777

© 2013 Wiley-VCH Verlag GmbH & Co. KGaA, Weinheim

NANO MICRO small

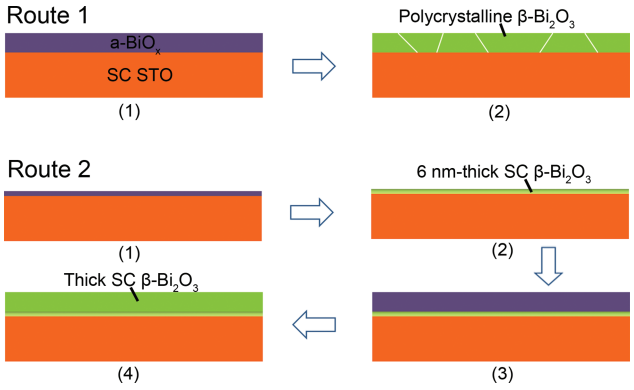

Figure 1. Two routes that lead to the formation of polycrystalline and SC β-Bi_2O_3 films, respectively. Route 1: (1) deposition of 100 nm BiO_x film followed by (2) crystallization operated at 500 °C for 3 h. Route 2 introduces a 6 nm thick SC β-Bi_2O_3 buffer layer: (1) deposition of a 6 nm thick BiO_x film; (2) annealing at 500 °C for 3 h, leading to the formation of a thin SC β-Bi_2O_3 buffer layer; (3) deposition of 100 nm BiO_x film; and (4) crystallization at 500 °C for 3 h. For route 2, from step (1) to step (2) is a heteroepitaxial growth, and from step (3) to step (4) is a homoepitaxial growth.

the film at 500 °C for 3 h (under which amorphous BiO_x would transform to β-Bi_2O_3) (Route 1 in **Figure 1**). Experimental results again indicated that the as-formed film was polycrystalline β-Bi_2O_3 (Figure S2(a)), similar to the results by using glass or silicon wafer as the substrate. After rinsing in diluted HCl solution, the β-Bi_2O_3 turned to a BiOCl film with a polycrystalline nature, and corresponding SEM image (Figure S2(b)) shows many BiOCl 2DONW domains in different orientations, confirming that the β-Bi_2O_3 film is polycrystalline. We also tried pulsed laser deposition followed by annealing, and still no SC β-Bi_2O_3 thin film was obtained. This is understood because a relatively thick epilayer will cause quite large stress and elastic energy, so that it finally forms a polycrystalline film, which can relax stress effectively.

When the film is thin enough, however, the result is quite different. We deposited a quite thin (only 6 nm thick) BiO_x film on STO substrate and annealed it at 500 °C for 3 h. It was then used as the substrate and covered with a 100 nm thick BiO_x film for crystallization (Route 2). The θ-2θ scan XRD spectrum in **Figure 2**(a) of the "two-layer" β-Bi_2O_3 film only shows a strong {002} reflection (except for the (001) peak of the STO substrate) (JCPDS 78-1793), indicating that it is single crystalline with the *c*-axis normal to the film plane. And this can explain the subsequent highly ordered superstructures of BiOCl shown in Figure 2(b)–(d), which will be discussed later on in details. To the best of our knowledge, this is the first report on a SC β-Bi_2O_3 (a metastable phase at room temperature) film. It is deduced that the 6 nm β-Bi_2O_3 film is single crystalline and plays the role of a buffer layer (also experimentally proved in Figure S2(a)), which effectively decreases the elastic energy of the system. And the crystallization of subsequent BiO_x film on the buffer layer is a homoepitaxy process, which is often easier than on a STO substrate. And that is why the 100 nm BiO_x film converts to a SC β-Bi_2O_3 film.

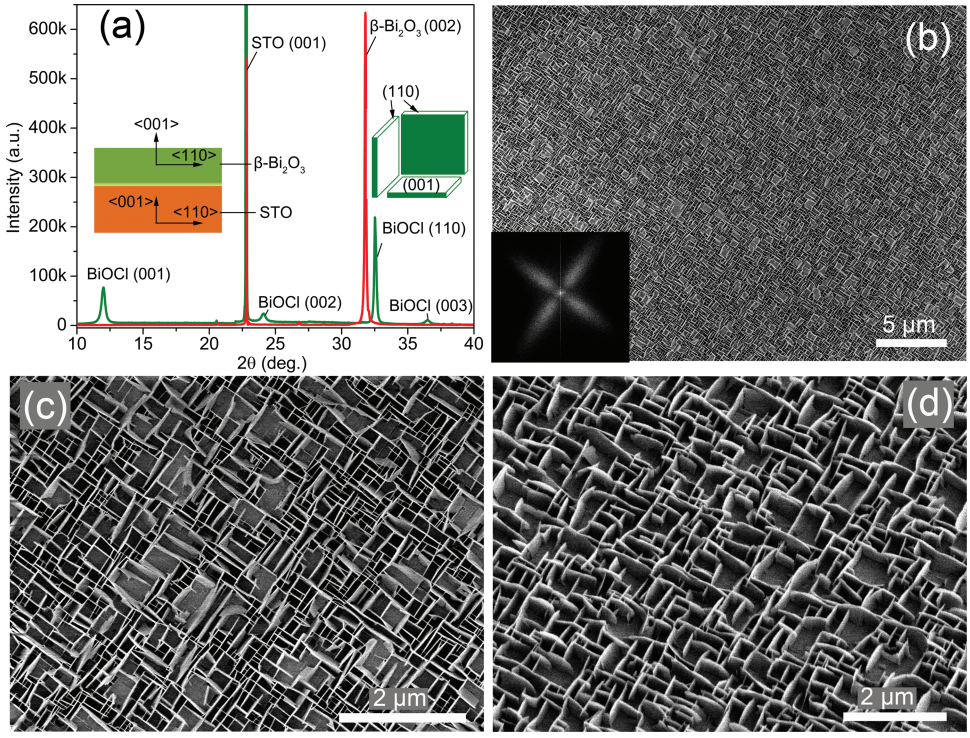

Figure 2. (a) XRD spectra of a SC β-Bi_2O_3/STO sample (red solid line), and corresponding BiOCl film (green solid line), which consists of three sets of mutually perpendicular nanoplate arrays. The left inset depicts the crystallographic orientations of the β-Bi_2O_3/STO heterojuction (corresponding to the red solid line of the XRD spectra), while the right inset shows that the BiOCl nanoplates are mutually perpendicular (corresponding to the green solid line). (b) and (c) Low and medium magnification SEM images of the BiOCl film (top view). Inset in panel (b) is a Fourier transformation pattern of the SEM image. (d) Corresponding tilt view.

© 2013 Wiley-VCH Verlag GmbH & Co. KGaA, Weinheim

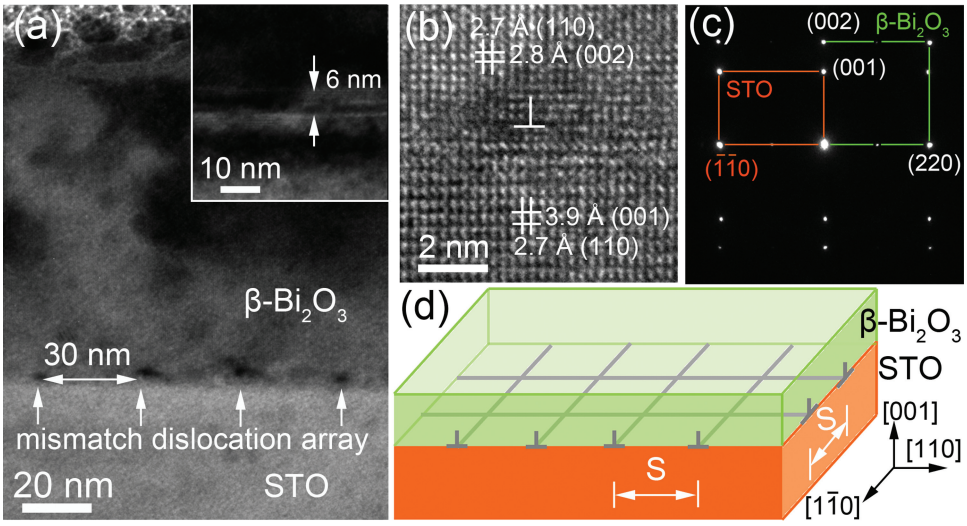

Figure 3. (a) Bright-field TEM image along the $[1\bar{1}0]$ zone axis of a slice obtained by FIB milling, showing a mismatch dislocation array in the β-Bi_2O_3/STO interface. Inset is a dark-field TEM image that clearly demonstrates a 6 nm thick β-Bi_2O_3 buffer layer. (b) Corresponding HRTEM image, showing a mismatch dislocation located at the β-Bi_2O_3/STO interface (the upper part is β-Bi_2O_3). (c) SAED pattern of the β-Bi_2O_3/STO interface, indicating that β-Bi_2O_3 grow on STO with $(001)_\beta \| (001)_{STO}$, and $(110)_\beta \| (110)_{STO}$. (d) Schematic of a β-Bi_2O_3 epilayer on STO, showing a mismatch dislocation network in the interface with a period of S.

The epilayer may have three possibilities of strain status. The first possibility is that the 6 nm thick β-Bi_2O_3 layer is a stress-free film. For this case, there should be a tetragonal network of misfit dislocations formed at the β-Bi_2O_3/STO interface with an interval of ~31.6 nm (this interval can be roughly calculated as $S = d_{110|STO}/f$). The second possibility is that the buffer layer is a fully strained film, and there is no mismatch dislocation. And the third possibility is a mixed case, in which only part of the strain is released by mismatch dislocations. In this case, mismatch dislocations might be found but the interval will be larger than 31.6 nm.

Our transmission electron microscopy (TEM) observation of a focused ion beam (FIB) milled specimen show a dislocation array with a period of ~30 nm (**Figure 3**(a)) along the $[1\bar{1}0]$ direction. However, this does not mean that the film is absolutely free of stress, because the dislocations themselves will also induce a stress field. Especially in our case, we could not accurately locate the dislocation cores (see the high resolution (HR) TEM image in Figure 3(b)), and the stress field may cover a large range to more than ten nanometers. The dark areas in the TEM image could roughly be regarded as the stress fields. Since β-Bi_2O_3 has a tetragonal structure, there should be another dislocation array in an equivalent case, along the [110] direction (Figure 3(d)), forming a tetragonal network of dislocations. Therefore, the thin β-Bi_2O_3 buffer layer has a high density of dislocations. Selected area electron diffraction (SAED) pattern and corresponding HRTEM image in Figure 3(b) and (c) show that β-Bi_2O_3 grows on STO with the c-axis out of plane, and the epitaxial relationship is: $(110)_\beta \| (110)_{STO}$, $(1\bar{1}0)_\beta \| (1\bar{1}0)_{STO}$, and $[001]_\beta \| [001]_{STO}$ (here the subscript 'β' indicates β-Bi_2O_3). The TEM analysis agrees well with the XRD results.

The SC β-Bi_2O_3 film could transform to 2DONW of BiOX (X = Cl and Br), $Bi_2O_2CO_3$, β-Bi_2O_3, or other bismuth compounds with a lattice parameter of $\sim 2^{n/2} \times 3.9$ Å ($n = 0, 1, 2, 3, 4$).[17] Here we only show BiOCl 2DONW because for other bismuth compounds the morphology is quite similar. Figure 2(b)–(d) are SEM images of a wafer scale (1 cm × 1 cm) BiOCl 2DONW transformed from a SC β-Bi_2O_3 film. These images clearly show that two sets of vertically aligned BiOCl nanowalls are grown perpendicular to each other on the STO substrate. The area of the 2DONW is limited only by the wafer. We inspected different zones of the sample and all demonstrated quite similar morphology and exactly the same orientations. Corresponding XRD diffraction spectrum (recorded by θ-2θ scan) in Figure 2(a) (the green solid line) reveals a strong BiOCl {110} peak, together with a set of relatively weak {00l} ($l = 1, 2, 3$) reflections. The structural information indicates that there are two sets of perpendicularly woven nanowalls grown vertically on the substrate (judged from the {110} peak), together with a set of tiled nanoplates (from the {00l} reflections). That is, there are three sets of mutually perpendicular nanowalls, vertical to or parallel to the STO surface. This is confirmed by the SEM images shown as in Figure 2(c) and (d), from which we can see a nanowall network and also some tiled nanoplates.

The morphology of the BiOCl 2DONW could be explained from the unique structure of β-Bi_2O_3. For the crystal structure of β-Bi_2O_3, it has two equivalent but perpendicular facets, (220) and $(2\bar{2}0)$, with a d-spacing of 2.737 Å in the [001] zone axis. And perpendicular to the (220) and $(2\bar{2}0)$ is the (002) facet, which has a quite close d-spacing of 2.817 Å. All of the facets can match the (110) or $(1\bar{1}0)$ facet of BiOCl ($d_{110} = 2.751$ Å), so that it is possible to form three sets of perpendicularly woven nanowalls. It can be figured out that one set of vertical BiOCl nanowalls are grown from β-Bi_2O_3 with $(1\bar{1}0)_{BiOCl} \| (002)_\beta$, $(110)_{BiOCl} \| (220)_\beta$, and $[001] \| [2\bar{2}0]$; and for the other vertical set in the perpendicular direction (indicated by "⊥"), it is $(1\bar{1}0)_{BiOCl\perp} \| (002)_\beta$, $(110)_{BiOCl\perp} \| (2\bar{2}0)_\beta$, and $[001]_{BiOCl\perp} \| [220]_\beta$. For the tiled BiOCl nanoplates, they are

© 2013 Wiley-VCH Verlag GmbH & Co. KGaA, Weinheim

NANO MICRO small

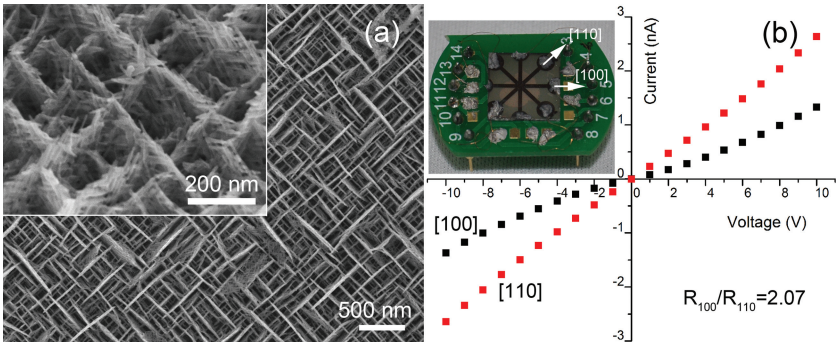

Figure 4. (a) SEM image of a Bi_2S_3 N2DONW, and inset is a high magnification tilt-view image, showing that each "nanowall" is actually a network of nanorods. (b) Current-voltage characteristic of Bi_2S_3 N2DONW, indicating that electrical conductivity along the [110] direction is twice that of the [100] direction. Here the crystal orientations are of the STO substrate rather than Bi_2S_3. The top left inset is an optical graph of the device.

grown from β-Bi_2O_3 with $(110)_{BiOCl}||(220)_{\beta}$, $(1\bar{1}0)_{BiOCl}||(2\bar{2}0)_{\beta}$, and $[001]_{BiOCl}||[002]_{\beta}$. And this can explain the XRD spectrum in Figure 2(a). Based on the above analysis, a β-Bi_2O_3 film with either the *c*- or the <110>-axis out of plane can lead to the formation of a 2DONW with three mutually perpendicular nanoplates (in this work, we have the β-Bi_2O_3 films with the *c*-axis out of plane).

The SC β-Bi_2O_3 could also transform to more complex superstructures such as Bi_2S_3 self-similar N2DONWs. For the Bi_2S_3 N2DONW, it is often transformed from BiOCl, BiOBr, $Bi_2O_2CO_3$, or β-Bi_2O_3 2DONW with lattice directing.[17] It consists of two levels structures. The first level is 2DONW of nanowalls. And for the second level, each nanowall is replaced with a tetragonal network of Bi_2S_3 nanorods along the [001] direction (**Figure 4**(a)). It is therefore a nested self-similar hierarchical structure. The Bi_2S_3 N2DONWs present apparently anisotropic physical properties related to the unique structure. For example, Figure 4(b) shows that the electrical conductivity along the [110] direction is almost twice that along the [100] direction, probably as a result of shorter path and weaker scattering (because of less joints) of electrons. It is apparent that the low resistance path is almost straight, while the high resistance path is zigzag and has more wall-to-wall joints as well. This is a demonstration that topological structure could affect physical properties of materials.

Besides β-Bi_2O_3 SC films, other SC films or bulks might also be potential for making 2DONWs of bismuth compounds. For example, NaCl has a cubic crystal structure with $a = 5.639$ Å, which is almost twice that of the d_{110} of BiOCl. A drop of $Bi(NO_3)_3$ solution on a (001)-oriented SC NaCl bulk can indeed result in BiOCl 2DONWs shown as in Figure S3. However, because NaCl is dissolvable, this process is not well controllable and BiOCl nanowalls are quite small.

With the β-Bi_2O_3 films, we are able to make superstructures of many kinds of bismuth compounds including β-Bi_2O_3 nanowall networks. Interestingly, when the SC β-Bi_2O_3 walls or plates are big enough, each wall might behave like a β-Bi_2O_3 film and transform to a 2DONW of BiOCl or N2DONW of Bi_2S_3, and if these large plates consists of a superstructure themselves it is then possible to make even more levels of ordered hierarchical nanostructures. Figure S4(a) shows two sets of vertically aligned BiOCl nanowall (which could finally transform to Bi_2S_3 network) formed on a large SC plate of β-Bi_2O_3, proving that such β-Bi_2O_3 single crystal can really act as the precursor for more complex hierarchical nanostructures. Figure S4(b)–(d) demonstrate two kinds of three-leveled Bi_2S_3 hierarchical nanostructures. The first level for panel (b) is stacked nanoplates, and for panels (c) and (d) is 2DONW, respectively; the second level is 2DONW; and the third level is the Bi_2S_3 network of nanorods. Such nanostructures are made up of oriented SC building blocks and possess quite large specific surface, so that they might be used in dye-sensitized solar cells, super capacitors, and lithium-ion batteries.

In conclusion, we have successfully obtained a SC β-Bi_2O_3 epilayer on STO by RF magnetron sputtering of amorphous BiO_x followed by annealing. An ultra-thin β-Bi_2O_3 film is introduced as a buffer layer that can effectively decrease the elastic energy of the system. The SC β-Bi_2O_3 epilayer could be transformed into a wafer scale network of β-Bi_2O_3, BiOX (X = Br, Cl), $Bi_2O_2CO_3$ nanowalls, and nested self-similar networks of Bi_2S_3 nanorods. The superstructures present special properties that are related to their unique morphologies, for example, the Bi_2S_3 nested networks show anisotropic electrical conductivity. This work may provide a platform for novel electronic and photoelectric devices.

Experimental Section

Preparation of Materials: BiO_x films were deposited on clean STO substrate by magnetron sputtering (ULVAC ACS4000-C4), with gas flow rates of 20 and 5 sccm for Ar and O_2, respectively. And crystallization was conducted at 500 °C for 3 h in a muffle furnace. SC β-Bi_2O_3 layer was obtained by a two-step process: we first deposited a 6 nm thick BiO_x film on STO, and after crystallization a 100 nm thick BiO_x film was again deposited onto it followed by crystallization. BiOCl 2DONW was synthesized by rinsing a SC β-Bi_2O_3 layer in diluted hydrochloric acid (0.2 M) for 1 min. $Bi_2O_2CO_3$ 2DONW was formed by incubating a SC β-Bi_2O_3 layer in blended solution of $NaHCO_3$ (0.04 M) and HNO_3 (0.02 M). β-Bi_2O_3 2DONW was prepared by annealing the $Bi_2O_2CO_3$ 2DONW at 320 °C for 1–3 days. And Bi_2S_3 N2DONW was obtained by incubating the β-Bi_2O_3 2DONW in blended solution of thioacetamide (0.04 M) and HCl (0.02 M) for two days.

Characterization: Morphology of the samples was observed by using a scanning electron microscope (Hitachi S4800). TEM images, HRTEM images and SAED patterns were recorded with a field emission transmission electron microscope (FEI Tecnai G^2 F20). XRD spectra were recorded with an X-ray diffractometer (Bruker D8 Focus). And I-V characteristic was measured with a Keithley 2635A source meter.

© 2013 Wiley-VCH Verlag GmbH & Co. KGaA, Weinheim

Supporting Information

Supporting Information is available from the Wiley Online Library or from the author.

Acknowledgements

C. F. Guo and J. Zhang contributed equally to this work. This work was supported by the funds from NSFC (10974037), NBRPC (2010CB934102), International S&T Cooperation Program (2010DFA51970) and Eu-FP7 (No. 247644). The authors thank Dr. K. Peng and Dr. X. Qi for assistance in FIB milling and TEM observations.

[1] G. Erik, P. Yang, *Nano Lett.* **2010**, *10*, 1082.
[2] K. Peng, X. Wang, S.-T. Lee, *Appl. Phy. Lett.* **2008**, *92*, 163103.
[3] C.-T. Huang, J. Song, W.-F. Lee, Y. Ding, Z. Gao, Y. Hao, L.-J. Chen, Z. L. Wang, *J. Am. Chem. Soc.* **2010**, *132*, 4766.
[4] X. Wang, J. Song, J. Liu, Z. L. Wang, *Science* **2007**, *316*, 102.
[5] H. Yan, R. He, J. Johnson, M. Law, R. J. Saykally, P. Yang, *J. Am. Chem. Soc.* **2003**, *125*, 4728.
[6] S. Fan, M. G. Chapline, N. R. Franklin, T. W. Tombler, A. M. Cassell, H. Dai, *Science* **1999**, *283*, 512.
[7] H. J. Fan, P. Werner, M. Zacharias, *Small* **2006**, *2*, 700.
[8] S. Tomohiro, T. Xie, J. Nishikawa, S. Shingubara, S. Senz, U. Gösele, *Adv. Mater.* **2007**, *19*, 917.
[9] H. J. Fan, W. Lee, R. Scholz, A. Dadgar, A. Krost, K. Nielsch, M. Zacharias, *Nanotechnology* **2005**, *16*, 913.
[10] S. Xu, Y. Wei, M. Kirkham, J. Liu, W. Mai, D. Davidovic, R. L. Snyder, Z. L. Wang, *J. Am. Chem. Soc.* **2008**, *130*, 14958.
[11] S. Conesa-Boj, E. Russo-Averchi, A. Dalmau-Mallorqui, J. Trevino, E. F. Pecora, C. Forestiere, A. Handin, M. Ek, L. Zweifel, L. R. Wallenberg, D. Rüffer, M. Heiss, Troadec David, L. D. Negro, P. Caroff, A. F. i Morral, *ACS Nano* **2012**, *6*, 10982.
[12] H. T Ng, J. Li, M. K. Smith, P. Nguyen, A. Cassell, J. Han, M. Meyyappan, *Science* **2003**, *300*, 1249.
[13] A. K. Geim, K. S. Novoselov, *Nat. Mater.* **2007**, *6*, 183.
[14] K. S. Novoselov, Z. Jiang, Y. Zhang, S. V. Morozov, H. L. Stormer, U. Zeitler, J. C. Maan, G. S. Boebinger, P. Kim, A. K. Geim, *Science* **2007**, *315*, 1379.
[15] L. Jiang, T. Yang, F. Liu, J. Dong, Z. Yao, C. Shen, S. Deng, N. Xu, Y. Liu, H. J. Gao, *Adv. Mater.* **2013**, *25*, 250.
[16] C. F. Guo, S. Cao, J. Zhang, H. Tang, Y. Tian, Q. Liu, *J. Am. Chem. Soc.* **2011**, *133*, 8211.
[17] C. F. Guo, J. Zhang, Y. Tian, Q. Liu, *ACS Nano* **2012**, *6*, 8746.
[18] L. Leontie, M. Caraman, M. Alexe, C. Harnagea, *Surf. Sci.* **2002**, *507*, 480.
[19] S. Cao, C. Guo, Y. Wang, J. Miao, Z. Zhang, Q. Liu, *Solid State Commun.* **2009**, *149*, 87.

Received: March 12, 2013
Revised: April 19, 2013
Published online: June 10, 2013

 © 2013 Wiley-VCH Verlag GmbH & Co. KGaA, Weinheim